Journal of Power Sources 205 (2012) 24–31

Contents lists available at SciVerse ScienceDirect

Journal of Power Sources

journal homepage: www.elsevier.com/locate/jpowsour

Platinum nanowire network with silica nanoparticle spacers for use as an oxygen reduction catalyst

Wataru Shimizu, Kazuyoshi Okada, Yoshitaka Fujita, ShanShan Zhao, Yasushi Murakami*

Division of Chemistry and Materials, Faculty of Textile Science and Technology, Shinshu University, 3-15-1 Tokida, Ueda, Nagano 386-8567, Japan

ARTICLE INFO

Article history:
Received 30 October 2011
Received in revised form 2 December 2011
Accepted 26 December 2011
Available online 3 January 2012

Keywords:
Polymer electrolyte membrane
Carbon free
Fuel cell
Colloidal silica
Rotating disk electrode
Oxygen reduction reaction

ABSTRACT

A platinum nanowire network (approximate ⌀4 nm) with silica nanoparticle (Pt_{net}/SiO_2) spacers was prepared via spray drying and hydrogen reduction. The large network had few grain boundaries of crystalline platinum and enclosed SiO_2 nanoparticles (average ⌀ 75 nm). These properties contributed to thermal and chemical stability of the structure. The nanowire network had a high electrochemical surface area ($31.3\ m^2\ g_{-Pt}^{-1}$), and acted as a catalyst for the oxygen reduction reaction. Its initial mass activity ($110.5\ A\ g_{-Pt}^{-1}$ at $0.85\ V_{RHE}$) was high compared to commercial Pt/C catalyst. Because of the chemical stability of the silica and the minimal amount of low-coordinated platinum in the platinum nanowires, Pt_{net}/SiO_2 retained 77% of its initial activity after 27 000 redox cycles compared to 57% for commercial Pt/C. We also demonstrate that the hydrogen peroxide generation from Pt_{net}/SiO_2 was less than half that from Pt/C.

1. Introduction

Platinum-based catalysts in polymer electrolyte membrane fuel cells efficiently convert electricity from hydrogen and oxygen at low temperature, and have attracted attention because of recent growth in the demand for alternative energy sources and environmental awareness [1,2]. Platinum nanoparticles (PtNPs) supported on carbon black (Pt/C) are commercially available and commonly used anode and cathode catalysts. Most recent studies have focused on development of cathode catalysts with high catalytic activities and durability for the oxygen reduction reaction (ORR) [2,3]. To increase the ORR activity, PtNPs (⌀ < 10 nm) loaded on an electrically conducting support with a high surface area, such as carbon black, are used to increase the reactive surface area of the platinum. During initial operation of the fuel cells, the catalytic activity reduced as the particle diameter increased from 3–4 nm to >5 nm because of dissolution and reprecipitation of the PtNPs [4–7]. Oxidative corrosion of the carbon support was also observed at applied potentials $>0.9\ V_{RHE}$, which resulted in aggregation of the PtNPs and a large decrease in the reactive surface area [7–10].

To increase the durability, alternative support materials have been investigated, including metal compounds with good electrical conductivity and chemical stability [11,12], and conducting metal oxides such as Ti_4O_7 [13,14], SnO_2 [15,16], RuO_2 [17], and sulfated ZrO_2 [18]. Ioroi et al. reported that PtNPs dispersed on a conducting titanium oxide, Ti_4O_7, exhibited catalytic activity as high as that of a commercial Pt/C catalyst with higher oxidative resistance [13]. Although conducting oxide supports avoid the corrosion problems, the electrical conductivities of these oxides are lower and they have reduced availability compared to carbon black.

In this research, we prepared a platinum nanowire network with silica nanoparticle spacers (Pt_{net}/SiO_2) via spray drying and hydrogen reduction. The use of a platinum nanowire network instead of PtNPs eliminated the need for a conducting support. We applied silica nanoparticles (average ⌀ 75 nm) to the support material of platinum nanowire networks owing to their excellent chemical stability and size uniformity. Preparation of the platinum nanowire networks by reduction with sodium borohydride has been studied with the aim of producing networks with few grain boundaries, smooth surfaces and low defects [19–23]. Although sodium borohydride is a mild reducing agent that is comparatively safe to handle in its solid form and can be used in aqueous or alcoholic solutions, hydrogen gas is a more economical reducing agent used for the preparation of metals in industry.

2. Experimental

2.1. Materials

Hydrogen hexachloroplatinate(IV) hexahydrate ($H_2PtCl_6{\cdot}6H_2O$, >99.9%) and 2-propanol (>99.7%) were purchased from Wako

* Corresponding author. Tel.: +81 268 21 5453; fax: +81 268 21 5477.
E-mail addresses: wats@shinshu-u.ac.jp (W. Shimizu), yasmura@shinshu-u.ac.jp (Y. Murakami).

0378-7753/$ – see front matter © 2012 Elsevier B.V. All rights reserved.
doi:10.1016/j.jpowsour.2011.12.053

Pure Chemical Industries (Osaka, Japan). Anhydrous ethylenediamine (>98%) was purchased from Tokyo Chemical Industry (Tokyo, Japan). PL-7 colloidal silica nanoparticles (SiO_2NPs) dispersed in water (average ⌀ 75 nm, silica mass fraction 23%) was obtained from Fuso Chemical (Osaka, Japan). Carbon black (EC300 J, 800 $m^2\,g^{-1}$) was received from Mitsubishi Chemical Corporation (Tokyo, Japan). As a control, commercial Pt/C catalyst (TEC10E50E, platinum mass fraction 46.4% on C Black EC-300J) was obtained from Tanaka Kikinzoku Kogyo (Tokyo, Japan). All chemicals were used as received.

2.2. Preparation of catalysts

For preparation of the platinum network, $H_2PtCl_6{\cdot}6H_2O$ was slowly dissolved in ethylenediamine to make sure the temperature did not rapidly increase. The clear yellow solution was kept in a tightly sealed bottle at 25 °C for 1 day, and during this time it turned into an opaque paste. 2-Propanol was added to adjust the platinum concentration to 0.132 mol L^{-1}. The solution was heated at 80 °C for 1 h, and then added to a nanoparticle dispersion of colloidal silica or carbon black dispersed in 2-propanol at room temperature. The platinum concentration in the nanoparticle dispersion was 0.066 mol L^{-1}, the molar ratio of $H_2PtCl_6{\cdot}6H_2O$ to ethylenediamine was 1–22.7, and silica was added at equal mass to the platinum. The mixture was stirred at 25 °C for 1 h and then sprayed onto a glass plate, which was heated to 105 °C to dry the nanoparticles without aggregation. A beige powder was obtained, and this was finely ground and reduced in a tube furnace with an Ar/H_2 (H_2 volume fraction 10%) gas stream at 270 °C for 2 h.

2.3. Structural and morphological characterization

A platinum mass fraction of yielded a black fine powder of Pt_{net}/SiO_2 or Pt_{net}/C was determined by means of an EX-200 energy-dispersive X-ray analyzer (Horiba, Kyoto, Japan). X-ray diffraction (XRD) measurements were conducted with a RINT2500HF X-ray diffractometer (Rigaku, Tokyo, Japan) with Cu Kα radiation (λ = 1.54056 Å). The diffractometer was operated at an accelerating voltage of 40 kV with a tube current of 40 mA. Diffraction patterns were collected at scanning angles between 20° and 90° with a scanning rate of 2° min^{-1} and a step size of 0.02°. The mean crystallite size, D, of platinum was calculated using the Scherrer formula $D = (0.9\lambda)/(\beta\cos\theta)$, where λ is the X-ray wavelength, β is the full-width at half-maximum expressed in radians, and θ is the diffraction angle of the crystalline phase determined at the peak maximum. Transmission electron microscope images of the Pt_{net}/SiO_2 and Pt_{net}/C powders were obtained using a JEM-2100 transmission electron microscope (JEOL, Tokyo, Japan) equipped with an UltraScan 1000 CCD camera (Gatan, Pleasanton, CA). The accelerating voltage was 200 kV. Finely ground powder was dispersed in methanol by ultrasonication. One drop of the suspension was placed on a 150 mesh carbon-coated copper grid, and then dried at 60 °C in air. A S-5000 scanning electron microscope (Hitachi, Tokyo, Japan) was used to examine the surface morphologies of the Pt_{net}/SiO_2 and Pt_{net}/C powders with a beam current of 10 μA and an acceleration voltage of 20 kV.

2.4. Electrochemical characterization

Electrochemical measurements were carried out using a three-electrode cell composed of a glassy carbon (GC) disk working electrode (⌀ 6 mm), a platinum mesh counter electrode, and a reversible hydrogen electrode as the reference electrode. The solution used for electrochemical measurements was 0.5 mol L^{-1} H_2SO_4 prepared from sulfuric acid (Wako Pure Chemical Industries, >96%) and Milli-Q deionized water (>18 MΩ, Millipore, Billerica, MA). The solution temperature was 60 °C. A HSV-100 potentiostat (Hokuto Denko, Tokyo, Japan) was used for potential control and recording data. Before the measurements, the GC working electrode was polished to a mirror-like finish with 1 and 0.05 μm alumina polishing suspensions (Baikowski, Annecy, France), and then washed with deionized water and ethanol. A Nafion® alcohol/water solution (Nafion mass fraction 5%, Sigma–Aldrich, St. Louis, MO) was diluted with ethanol (Wako Pure Chemical Industries, >99.5%) to one three-hundredth of the original concentration, and 10 μL of the dilute solution was coated on the GC electrode. Catalyst powder (10 mg) was dispersed in a water/ethanol mixture to a concentration of 1 g L^{-1}. An aliquot (10 μL) of this homogeneous dark dispersion was dropped onto the Nafion layer on the GC electrode. This embedded the catalyst in the semidry Nafion layer. After drying at 80 °C for 45 min, the Pt loading on the working electrode was 17.7 μg cm^{-2}.

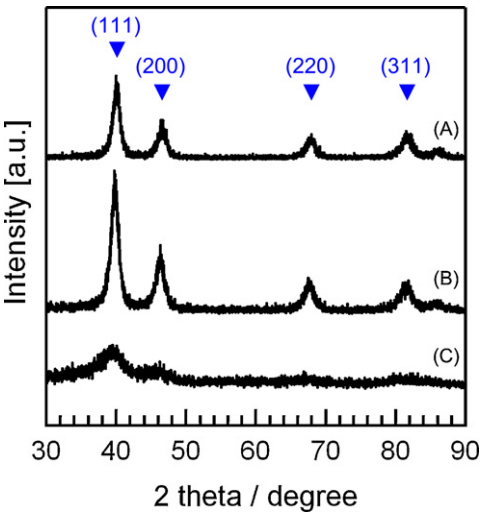

Fig. 1. XRD patterns of synthesized Pt_{net}/SiO_2 (A) and Pt_{net}/C (B) and commercial Pt/C (C) powders. The peaks are marked with triangles labeled with the Miller indices, (*hkl*), for the face centered cubic crystal.

Cyclic voltammograms (CVs) were measured in N_2-bubbled electrolyte solution at a scan rate of 50 mV s^{-1} between 0.05 and 1.20 V_{RHE}. The electrochemical surface area of the platinum in each of the catalysts was derived from hydrogen desorption charges estimated from the CVs [24–26]. Rotating disk electrode experiments were performed to evaluate the catalytic activity for the ORR [27–30]. The working electrode was mounted on a rotating disk electrode holder equipped with a rotation speed controller (Nikko Keisoku, Atsugi, Japan). Linear sweep voltammetry measurements were conducted in O_2-saturated electrolyte at a scan rate of 5 mV s^{-1} from 1.05 to 0.05 V_{RHE} with rotation rates between 1000 and 3000 rpm. The data obtained at all rotation rates were used for Koutecky–Levich analysis [31–33]. Before these measurements, the catalyst surface was activated by 20 cyclic scans at a scan rate of 50 mV s^{-1} between 0.05 and 1.20 V_{RHE}.

Accelerated degradation tests were conducted on the three-electrode cell with the O_2-saturated 0.5 mol L^{-1} H_2SO_4 electrolyte solution at 60 °C. The composition of the testing cell was same as described above except that a Au disk (⌀ 6 mm) was used as the working electrode in place of the GC disk. Scans were repeated 27 000 times with a scanning rate of 100 mV s^{-1} between 0.8 and 1.30 V_{RHE}. The CVs and linear sweep voltammograms were determined after each scan.

Hydrogen peroxide generated during oxygen reduction was detected by Rotating ring-disk electrode (RRDE) measurements using a platinum ring (1 mm width) and GC disk (⌀ 6 mm) electrode.

Table 1
Summary of the catalyst properties[a].

Sample	w_{pt} (%)	$D_{(1\,1\,1)}$ (nm)	S ($m^2\,g_{\text{-Pt}}^{-1}$)	j_k at 0.85 V_{RHE} (mA $cm_{\text{-Pt}}^{-2}$)	$j_{k\text{-mass}}$ at 0.85 V_{RHE} (A $g_{\text{-Pt}}^{-1}$)
Pt_{net}/Si_2	51.1	13.9	27.9	0.415	115.8
Pt_{net}/C	48.8	14.3	28.5	0.358	102.0
Pt/C (commercial)	46.4	4.2	56.6	0.155	103.4

[a] Notation: w_{pt}, Pt mass fraction determined from the EDX analysis except Pt/C (commercial); $D_{(111)}$, Pt crystallite diameter calculated using the Scherrer equation with full width at half maximum of the (1 1 1) peak; S, electrochemical surface area (ESA) calculated from hydrogen desorption charges; j_k, specific activity given as kinetic current density in Koutecky–Levich plots; $j_{k\text{-mass}}$, mass activity calculated from j_k and ESA. All electrochemical measurements were conducted using a glassy carbon disc electrode.

Before the measurements, the ring-disk electrode was polished as described above for the disk electrode. An aliquot (10 μL) of the catalyst dispersion was dropped onto the semidry Nafion layer on the GC disk electrode, and this step was repeated several times to prepare electrodes with different amounts of the catalysts. The O_2-saturated 0.1 mol L^{-1} $HClO_4$ electrolyte solution was prepared from perchloric acid (Wako Pure Chemical Industries, 60%) and Milli-Q deionized water and kept at 60 °C. Data were collected with an AUTOLAB PGSTAT 12 potentiostat (Metrohm Autolab B. V., Utrecht, The Netherlands). The catalyst surface was stabilized by 20 scan cycles between 0.05 and 1.20 V_{RHE} at 50 mV s^{-1}. The GC disk electrode was swept at 5 mV s^{-1} from 0.05 to 1.02 V_{RHE} while rotating the ring-disk electrode at 2000 rpm and holding the platinum ring electrode at 1.0 V_{RHE}.

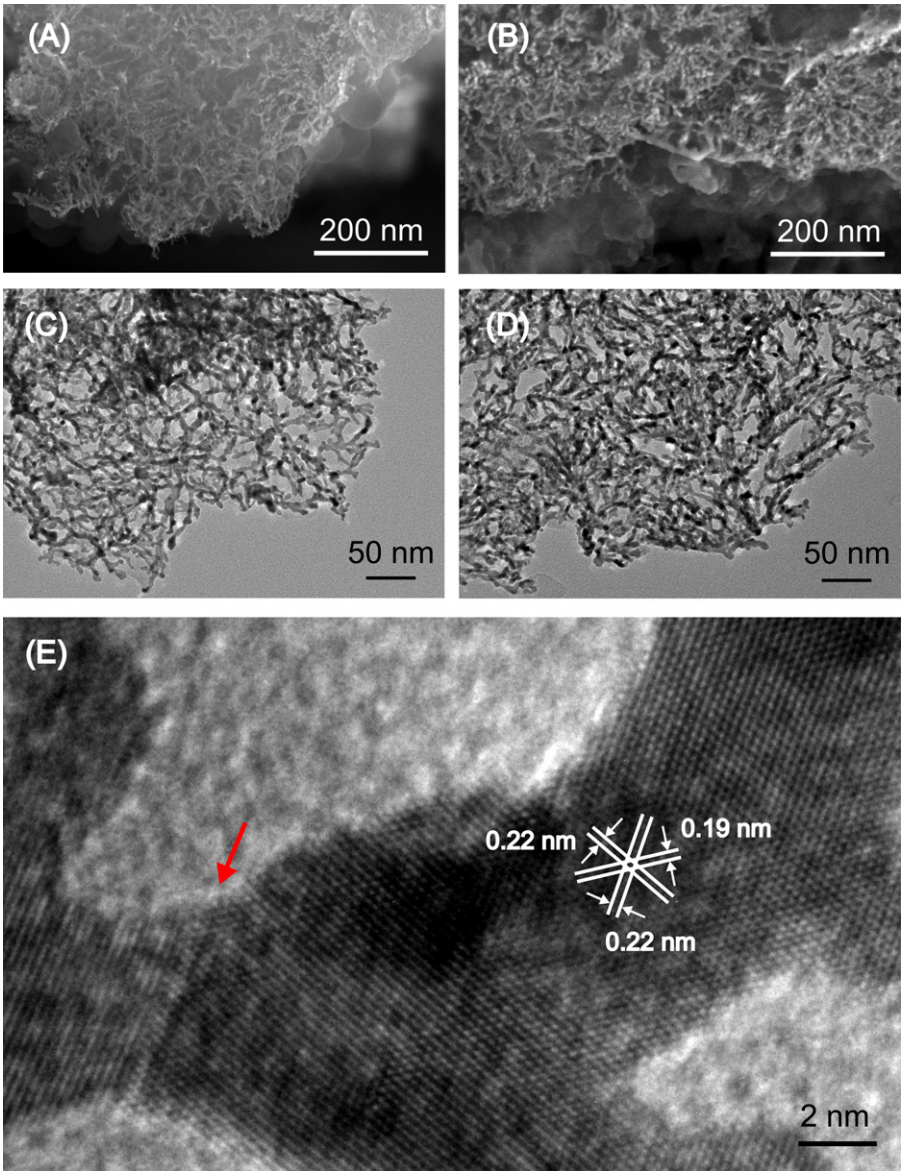

Fig. 2. Scanning electron microscopy images of Pt_{net}/SiO_2 (A) and Pt_{net}/C (B), transmission electron microscopy images of Pt_{net}/SiO_2 (C) and Pt_{net}/C (D), and a typical magnified transmission electron microscopy image of the networked platinum (E). The red arrow indicates the location of a grain boundary. (For interpretation of the references to color in this figure legend, the reader is referred to the web version of the article.)

Table 2
Summary of the catalyst properties for the cycle test[a].

Sample	S (m^2 g_{-Pt}^{-1})		j_k at 0.85 V_{RHE} (mA cm_{-Pt}^{-2})		$j_{k\text{-mass}}$ at 0.85 V_{RHE} (A g_{-Pt}^{-1})	
	Initial[b]	Last[c]	Initial	Last	Initial	Last
Pt_{net}/SiO_2	31.3	29.8	0.37	0.28	110.5	84.8
Pt_{net}/C	26.9	20.4	0.39	0.34	105.9	70.1
Pt/C (commercial)	58.3	29.0	0.17	0.20	100.2	57.0

[a] Notation: S, electrochemical surface area (ESA) calculated from hydrogen desorption; j_k, specific activity given as kinetic current density in Koutecky–Levich plots; $j_{k\text{-mass}}$, mass activity calculated from j_k and ESA. The data were collected [b]before and [c]after the cycle tests. All electrochemical measurements were conducted using a Au disc electrode.

3. Results and discussion

3.1. Structures and morphologies of the platinum nanowire networks

Platinum mass fraction of Pt_{net}/SiO_2 and Pt_{net}/C was 50%. The XRD patterns of the Pt_{net}/SiO_2 and Pt_{net}/C catalysts and a commercial Pt/C catalyst confirmed the platinum crystal structure was face-centered cubic (Fig. 1). Peaks attributed to (1 1 1), (2 0 0), (2 2 0) and (3 1 1) reflections were stronger in the diffraction patterns of the Pt_{net}/SiO_2 and Pt_{net}/C catalysts than in that of the commercial Pt/C catalyst. The crystalline sizes were estimated from the full widths at half maximum of the peaks, and those for Pt_{net}/SiO_2 (13.9 nm) and Pt_{net}/C (14.3 nm) were much larger than that of commercial Pt/C (4.2 nm) (Table 1).

Scanning electron microscopy images of Pt_{net}/SiO_2 and Pt_{net}/C revealed that the thin platinum nanowire network was spaced by the SiO_2NPs (approximate ⌀ 70 nm) (Fig. 2(A) and (B)). The conducting platinum nanowire network prevented the electron from charging during scanning electron microscopy. The platinum nanowire networks of Pt_{net}/SiO_2 and Pt_{net}/C were also observed by transmission electron microscopy (Fig. 2(C) and (D)). The average diameter of the platinum nanowires in Pt_{net}/SiO_2 (4.5 nm) was less than that of the platinum nanowires in Pt_{net}/C (5.2 nm). The platinum nanowire slightly flattened in shape, like a ribbon rather than a rod. A magnified image of Pt_{net}/SiO_2 revealed continuous crystal growth of platinum with interplanar distances (0.19 nm for {2 0 0} and 0.22 nm for {1 1 1}) consistent with the face centered cubic platinum structure (Fig. 2(E)). The platinum nanowire networks of the prepared catalysts were more complex than platinum nanowire networks prepared by liquid-phase reduction using sodium borohydride [19,21,22,34], and showed branching and crossing of the nanowires. Because of the branched nanowires, the platinum nanowire network had high density. Moreover, the continuous crystal growth contributed to the presence of few grain boundaries. These unique configurations gave the network high electrical conductivity.

3.2. Comparison of electrochemical properties

The CVs of Pt_{net}/SiO_2 and Pt_{net}/C showed characteristic double anodic current peaks at approximately 0.12 and 0.25 V_{RHE} (Figs. 3(A) and 4(A)). These peaks could be attributed to hydrogen desorption from the platinum surface on the (1 1 0) plane (0.12 V_{RHE}) and (1 0 0) plane (0.25 V_{RHE}) [35]. The peak shapes for the platinum nanowire networks were similar to that of Pt black [36] and Pt/C, which indicates that the platinum nanowire networks consist of polycrystalline platinum [37]. For commercial Pt/C, a third anodic current peak was observed between those at 0.12 and 0.25 V_{RHE} (Fig. 4(D)), which can be attributed to the high content of platinum atoms with low surface coordination in the PtNPs [35,38]. By contrast, this peak was not observed for the platinum nanowire networks, which indicates they contain few platinum atoms with low surface coordination.

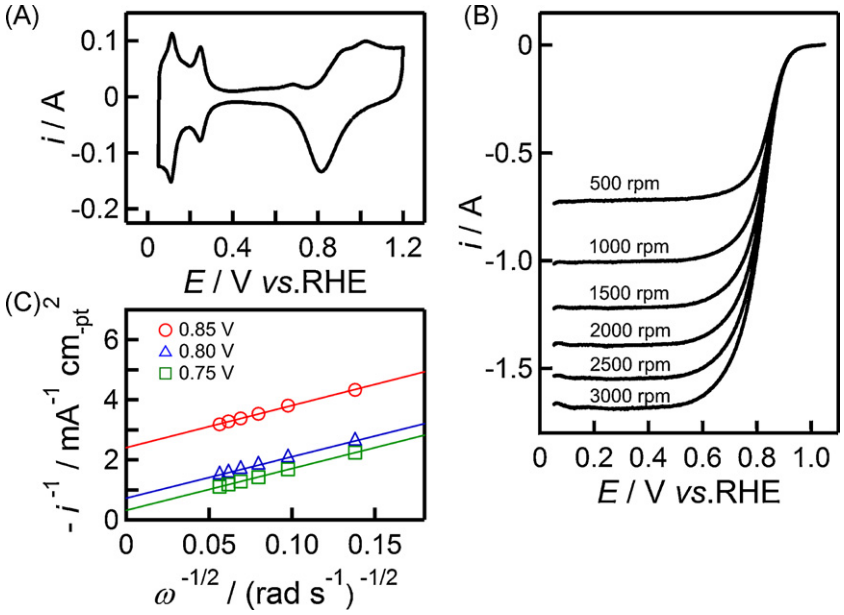

Fig. 3. Electrochemical properties of the Pt_{net}/SiO_2 catalyst. (A) A cyclic voltammogram measured in a N_2-saturated electrolyte solution of 0.5 mol L^{-1} H_2SO_4 at 60 °C with a scan rate of 50 mV s^{-1}, (B) linear sweep voltammograms measured in O_2-saturated electrolyte solution of 0.5 mol L^{-1} H_2SO_4 at 60 °C with a scan rate of 5 mV s^{-1}, and (C) Koutecky–Levich plots using extracted data from the kinetic ORR currents at 0.85 V_{RHE} (red circle), 0.80 V_{RHE} (blue triangle), and 0.75 V_{RHE} (green square). (For interpretation of the references to color in this figure legend, the reader is referred to the web version of the article.)

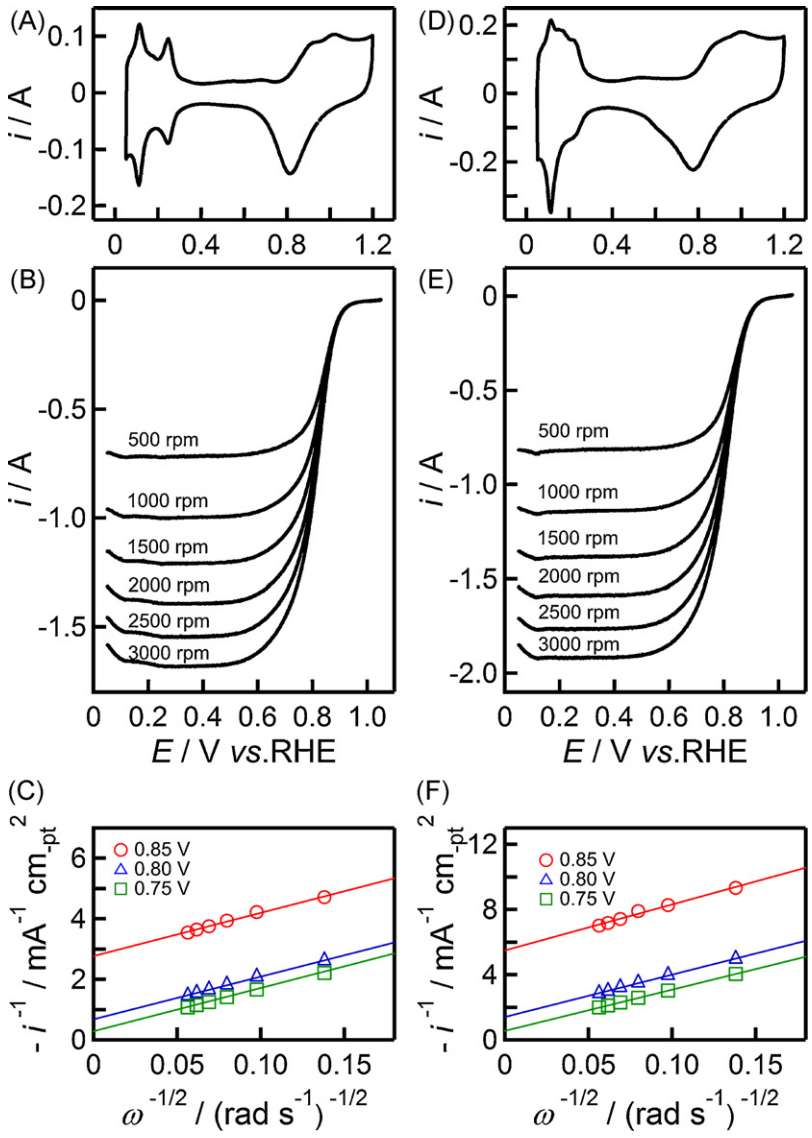

Fig. 4. Electrochemical properties of the Pt_{net}/C (left) and commercial Pt/C catalysts (right). (A) and (D) Cyclic voltammograms measured in a N_2-saturated electrolyte solution of 0.5 mol L^{-1} H_2SO_4 at 60 °C with a scan rate of 50 mV s^{-1}, (B) and (E) linear sweep voltammograms measured in an O_2-saturated electrolyte solution of 0.5 mol L^{-1} H_2SO_4 at 60 °C with a scan rate of 5 mV s^{-1}, and (C) and (F) Koutecky–Levich plots using extracted data from the kinetic ORR currents at 0.85 V_{RHE} (red circle), 0.80 V_{RHE} (blue triangle), and 0.75 V_{RHE} (green square). (For interpretation of the references to color in this figure legend, the reader is referred to the web version of the article.)

The electrochemical surface areas (ESA) of Pt_{net}/SiO_2 and Pt_{net}/C were half that of the commercial Pt/C catalyst (Table 1). Independence of the electrical conductivity of the support, such as silica and carbon black, suggests that the platinum nanowire network itself is electrically conductive. Even though the Pt_{net}/SiO_2 (13.9 nm) and Pt_{net}/C (14.3 nm) had large crystalline sizes (estimated by XRD), the ESA were quite high because the networks are made of fine platinum nanowires (⌀ 4 nm). The ESA of a support-free platinum nanowire network catalyst, 21.8 m^2 g_{-pt}^{-1}, derived from the platinum precursor solution containing no SiO_2NPs was smaller than the ESA of Pt_{net}/SiO_2, 27.9 m^2 g_{-pt}^{-1}. The data imply that the SiO_2NPs acted as a spacer inhibiting densification during the crystal growth of platinum through the calcination and reduction process.

Kinoshita indicated that the number of the edge and corner sites decreased with increasing platinum particle size [39]. Low coordination platinum atoms are exposed at edges and corners. We consider that large crystal size and diameter of the platinum nanowire networks decreased these sites. Also, from TEM images (Fig. 2(C) and (D)), the flat surface of the platinum nanowire network were expected to decrease the edge and corner sites.

Koutecky–Levich plots (Fig. 3(B)) were constructed from linear sweep voltammograms measured using a GC disc (⌀ 6 mm) electrode at rotation rates between 500 and 3000 rpm (Fig. 3(C)). The mass activity, $j_{k\text{-mass}}$, of Pt_{net}/SiO_2 (115.8A g_{-Pt}^{-1} at 0.85 V_{RHE}) was higher than that of commercial Pt/C (103.4A g_{-Pt}^{-1} at 0.85 V_{RHE}). Because Pt_{net}/SiO_2 had half the ESA of the commercial catalyst but higher mass activity, its specific activity, j_k (0.415 mA cm_{-Pt}^{-2} at 0.85 V_{RHE}) was twice that of the commercial Pt/C (0.155 mA cm_{-Pt}^{-2} at 0.85 V_{RHE}). The j_k of Pt_{net}/C (0.358 mA cm_{-Pt}^{-2} at 0.85 V_{RHE}) was relatively low compared to that of Pt_{net}/SiO_2 even though the platinum nanowire network was identical. The specific activity depends on surface properties of platinum, such as an electronic state and a coordination number, and is affected by the chemical characteristics of the support [40] and the number of platinum atoms, i.e., particle size [39,41]. The large crystal size of platinum of Pt_{net}/SiO_2 and Pt_{net}/C would contribute to the high specific activity of ORR [42].

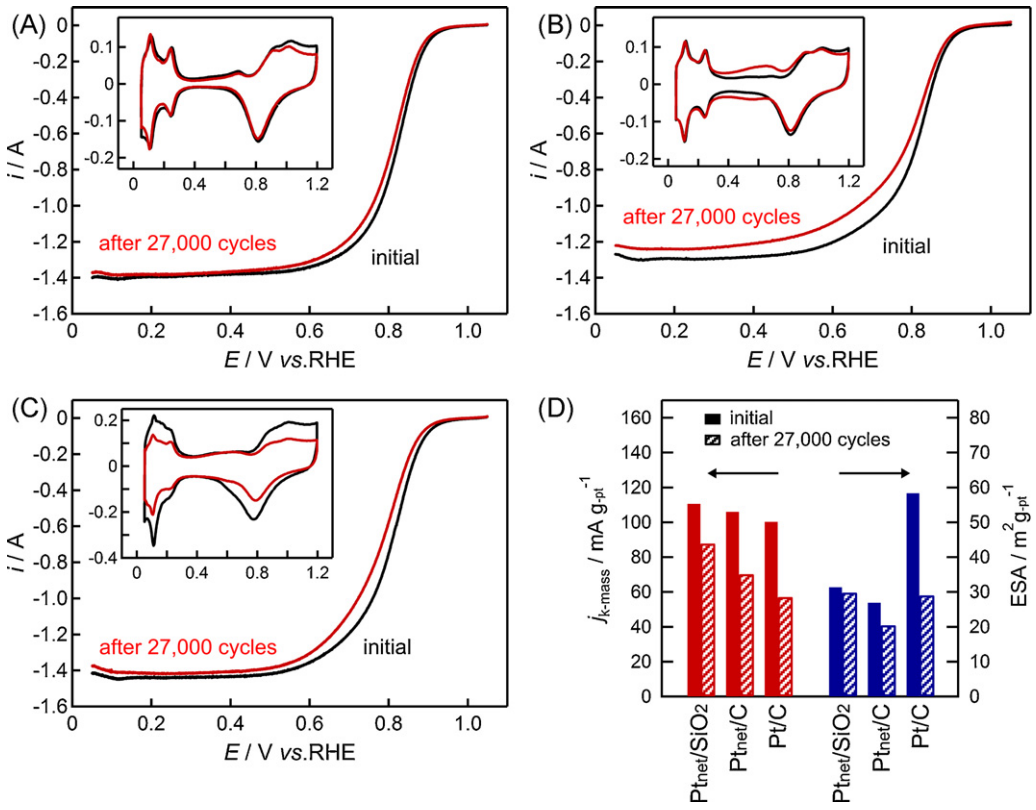

Fig. 5. Comparison of the linear sweep voltammograms and cyclic voltammograms (inset) before (black) and after (red) accelerated degradation testing for the Pt_{net}/SiO_2 (A), Pt_{net}/C (B), and commercial Pt/C (C) catalysts, and comparison of the ORR mass activities (red) and ESAs (blue) of each catalyst (D). Linear sweep voltammograms were measured in an O_2-saturated electrolyte solution of 0.5 mol L^{-1} H_2SO_4 at 60 °C with a scan rate of 5 mV s^{-1} and electrode rotation rate of 2000 rpm. Cyclic voltammograms were measured in a N_2-saturated electrolyte solution of 0.5 mol L^{-1} H_2SO_4 at 60 °C with a scan rate of 50 mV s^{-1}. (For interpretation of the references to color in this figure legend, the reader is referred to the web version of the article.)

3.3. Durability studies of platinum nanowire networks

Accelerated durability testing (ADT) of Pt_{net}/SiO_2 (Fig. 5(A)) was carried out by 27 000 repeat cyclic voltammetry scans between 0.8 and 1.3 V_{RHE} at a scanning rate of 100 mV s^{-1}. The results were compared to those for commercial Pt/C (Fig. 5(C)). To avoid electrode corrosion, a Au rotation electrode was used for the ADT instead of the glassy carbon electrode that is widely used for fuel cell catalysts. The ESA of Pt_{net}/SiO_2 decreased by 4% after the ADT, whereas that of Pt_{net}/C (Fig. 5(B)) decreased by 23% (Table 2). These reductions were attributed to oxidative corrosion of the carbon support, which would partially collapse the platinum nanowire network. Oxidation of the carbon supports was reflected the increase in double layer capacitance between about 0.4 and 0.6 V_{RHE} with repetition of the cyclic voltammetry of Pt_{net}/C and commercial Pt/C [43,44]. The use of SiO_2NPs stabilized the platinum nanowire network during ORR. We attribute the high durability of Pt_{net}/SiO_2 to the stability of the silica support against corrosion and of the platinum nanowire network structure during ORR.

The ESA of the commercial Pt/C decreased by >50% (Fig. 5 (D)), and this was much larger than the decrease for Pt_{net}/C (23%). This difference between the catalysts could arise from the degree of platinum dissolution. The PtNPs in commercial Pt/C have a high concentration of low-coordination platinum edge sites, which are more likely to dissolve during potential cycling [4,6,45]. The low-coordination platinum edge sites would be easily oxidized with the oxygen species, gradually producing dissoluble platinum ion during the oxidation–reduction cycles. The platinum nanowire network has a low concentration of low-coordination platinum edge sites, which is advantageous over the PtNPs because it stops platinum dissolution during the redox cycle.

The $j_{k\text{-mass}}$ of Pt_{net}/SiO_2 decreased by 23%, and with the small ESA decrease for this catalyst the $j_{k\text{-mass}}$ decrease could be attributed to the j_k decrease (38%). By contrast, larger decreases in the $j_{k\text{-mass}}$ of Pt_{net}/C (34%) and commercial Pt/C (43%) were observed, and with the slight j_k changes for these catalysts the $j_{k\text{-mass}}$ decrease could be attributed to their ESA decreases. The j_k decrease for Pt_{net}/SiO_2 would be caused by changes in the state of the platinum on the inside of the structure during ORR. The j_k of Pt_{net}/C, which had the same platinum nanowire network, remained constant even after the ADT, whereas its ESA decreased. The j_k decrease of platinum strongly depended on its surface and sub-surface state. Changes in the state of the platinum on the inside of the structure occur through processes at the platinum surface, such as diffusion of oxygen species into subsurfaces of the bulk platinum [46,47].

3.4. Selectivity of oxygen reduction on platinum nanowire networks

The electrocatalytic activities of the Pt_{net}/SiO_2 and commercial Pt/C catalysts toward the reduction of oxygen to hydrogen peroxide were evaluated using the ring-disk electrode [29,48]. Hydrogen peroxide molecules generated from a platinum catalyst on the disk electrode will diffuse through the electrolyte to the ring electrode, where the hydrogen peroxide is oxidized to water. The magnitude of the ring current reflects the amount of hydrogen peroxide decomposed on the ring electrode. In large quantities, the platinum catalysts considerably decreased the ring current (Fig. 6). Hydrogen peroxide was partially decomposed to water over the platinum catalysts on the disk electrode during diffusion to the ring electrode [49]. High ring currents were observed with the Pt_{net}/SiO_2 (1.0 μg_{-Pt}) and the commercial Pt/C (0.5–1.0 μg_{-Pt}) catalysts over

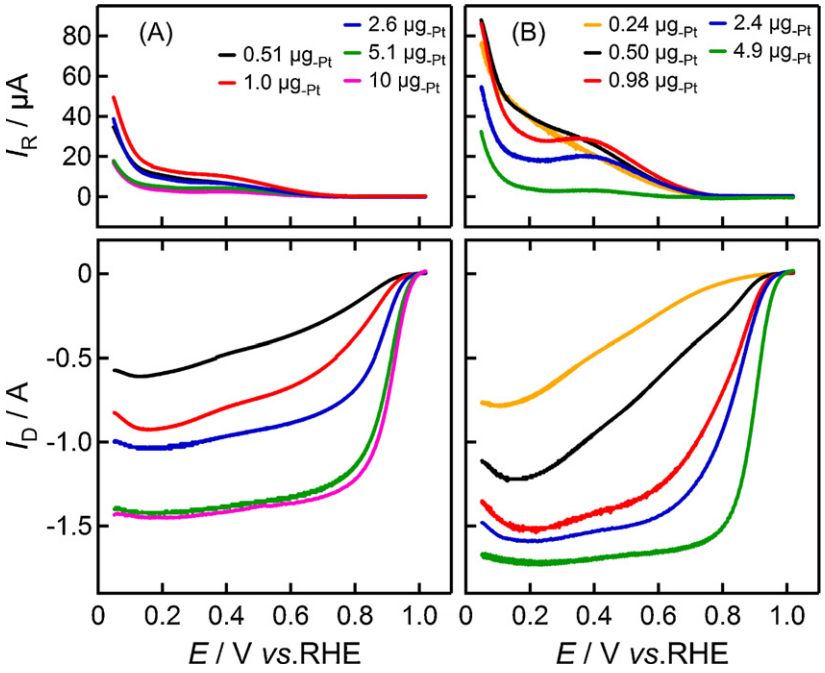

Fig. 6. Ring, I_R, (top) and disk, I_D, (bottom) currents of different quantities of the Pt_{net}/SiO_2 (A) and commercial Pt/C (B) catalysts loaded on the GC disk electrode during ORR in an O_2-saturated electrolyte solution of 0.1 mol L^{-1} $HClO_4$ at 60 °C. The potential of the GC disk electrode was swept at 5 mV s^{-1} from 0.05 to 1.02 V_{RHE} with rotating the ring-disk electrode at 2000 rpm, while the platinum ring electrode was held at 1.0 V_{RHE}.

a wide potential range (0.05–0.6 V_{RHE}), and the influence of catalytic decomposition of hydrogen peroxide would be small. When the ring currents of these catalysts were compared at an arbitrary potential below 0.6 V_{RHE}, the ring current of Pt_{net}/SiO_2 (1.0 μg_{-Pt}) was less than the half that of the commercial Pt/C catalyst (0.5 and 1.0 μg_{-Pt}). These results imply that the platinum nanowire network in the Pt_{net}/SiO_2 prevents hydrogen peroxide from forming, unlike the PtNPs in the commercial Pt/C catalyst. This phenomenon was especially notable at low potentials (<0.4 V_{RHE}). The characteristics of hydrogen peroxide generation on the Pt_{net}/C catalyst were similar to those for the Pt_{net}/SiO_2 catalyst, and this was confirmed by the RRDE experiments. We believe that the higher j_k for Pt_{net}/SiO_2 and Pt_{net}/C (Table 1) is because of the low selectivity for hydrogen peroxide generation in the oxygen reduction reaction.

Bridge site adsorption of an oxygen molecule will occur on the flat platinum surface of the platinum nanowire network in Pt_{net}/SiO_2 and Pt_{net}/C, which helps dissociation of oxygen into oxygen atoms and the four-electron ORR into water. Bidentate site adsorption on the low-coordination platinum edge site in the commercial Pt/C catalyst will prevent the oxygen molecule from dissociating, which favors hydrogen peroxide formation via the two-electron ORR. The decrease in hydrogen peroxide formation will prevent decreases in the cell performance that are caused by polymer membrane decomposition because of hydrogen peroxide [7,50].

4. Conclusions

Platinum nanowire (⌀ 4 nm) networks with SiO_2NP spacers were synthesized by reduction using H_2 gas instead of metal borohydride. These networks exhibited higher electrocatalytic activity and durability for the ORR then commercial Pt/C. The high ORR mass activity of Pt_{net}/SiO_2 could be attributed to its high specific activity per platinum surface area compared to the PtNPs. The use of SiO_2NPs stabilized the platinum nanowire network during both calcination and H_2 reduction in the catalyst preparation and ORR. After ADT of Pt_{net}/SiO_2, the ESA remained constant and the mass activity decreased by 23.2%. This decrease was much smaller than that of commercial Pt/C (43.1%). The selectivity of the ORR for hydrogen peroxide on Pt_{net}/SiO_2 was lower than that on the commercial Pt/C. The decrease in the hydrogen peroxide formation is also expected to increase the durability of polymer membranes.

Acknowledgements

This work was supported by the Program for Fostering Regional Innovation in Nagano, granted by the Ministry of Culture, Education, Sports, Science and Technology, Japan.

References

[1] B.C.H. Steele, A. Heinzel, Nature 414 (2001) 345–352.
[2] H.A. Gasteiger, S.S. Kocha, B. Sompalli, F.T. Wagner, Appl. Catal. B: Environ. 56 (2005) 9–35.
[3] P. Mani, R. Srivastava, P. Strasser, J. Phys. Chem. C 112 (2008) 2770–2778.
[4] K. Kinoshita, J.T. Lundquis, P. Stonehart, J. Electroanal. Chem. Interfacial Electrochem. 48 (1973) 157–166.
[5] K. Yasuda, A. Taniguchi, T. Akita, T. Ioroi, Z. Siroma, Phys. Chem. Chem. Phys. 8 (2006) 746–752.
[6] X.P. Wang, R. Kumar, D.J. Myers, Electrochem, Solid State Lett. 9 (2006) A225–A227.
[7] R. Borup, J. Meyers, B. Pivovar, Y.S. Kim, R. Mukundan, N. Garland, D. Myers, M. Wilson, F. Garzon, D. Wood, P. Zelenay, K. More, K. Stroh, T. Zawodzinski, J. Boncella, J.E. McGrath, M. Inaba, K. Miyatake, M. Hori, K. Ota, Z. Ogumi, S. Miyata, A. Nishikata, Z. Siroma, Y. Uchimoto, K. Yasuda, K. Kimijima, N. Iwashita, Chem. Rev. 107 (2007) 3904–3951.
[8] E. Antolini, J. Mater. Sci. 38 (2003) 2995–3005.
[9] I.M. Roen, C.H. Paik, T.D. Jarvi, Electrochem. Solid-State Lett. 7 (2004) A19–A22.
[10] S. Maass, F. Finsterwalder, G. Frank, R. Hartmann, C. Merten, J. Power Sources 176 (2008) 444–451.
[11] Y.Y. Shao, J. Liu, Y. Wang, Y.H. Lin, J. Mater. Chem. 19 (2009) 46–59.
[12] E. Antolini, E.R. Gonzalez, Solid State Ionics 180 (2009) 746–763.
[13] T. Ioroi, Z. Siroma, N. Fujiwara, S. Yamazaki, K. Yasuda, Electrochem. Commun. 7 (2005) 183–188.
[14] G.Y. Chen, S.R. Bare, T.E. Mallouk, J. Electrochem. Soc. 149 (2002) A1092–A1099.
[15] A.L. Santos, D. Profeti, P. Olivi, Electrochim. Acta 50 (2005) 2615–2616.
[16] A. Masao, S. Noda, F. Takasaki, K. Ito, K. Sasaki, Electrochem. Solid-State Lett. 12 (2009) B119–B122.
[17] K. Lasch, G. Hayn, L. Jorissen, J. Garche, O. Besenhardt, J. Power Sources 105 (2002) 305–310.

[18] Y. Suzuki, A. Ishihara, S. Mitsushima, N. Kamiya, K. Ota, Electrochem. Solid-State Lett. 10 (2007) B105–B107.
[19] Y. Song, R.M. Garcia, R.M. Dorin, H.R. Wang, Y. Qiu, E.N. Coker, W.A. Steen, J.E. Miller, J.A. Shelnutt, Nano Lett. 7 (2007) 3650–3655.
[20] A. Chen, P. Holt-Hindle, Chem. Rev. 110 (2010) 3767–3804.
[21] C. Koenigsmann, W.P. Zhou, R.R. Adzic, E. Sutter, S.S. Wong, Nano Lett. 10 (2010) 2806–2811.
[22] S.Y. Wang, S.P. Jiang, X. Wang, J. Guo, Electrochim. Acta 56 (2011) 1563–1569.
[23] E. Antolini, J. Perez, J. Mater. Sci. 46 (2011) 4435–4457.
[24] M.K. Min, J.H. Cho, K.W. Cho, H. Kim, Electrochim. Acta 45 (2000) 4211–4217.
[25] Y.H. Shih, G.V. Sagar, S.D. Lin, J. Phys. Chem. C 112 (2008) 123–130.
[26] K.J.J. Mayrhofer, D. Strmcnik, B.B. Blizanac, V. Stamenkovic, M. Arenz, N.M. Markovic, Electrochim. Acta 53 (2008) 3181–3188.
[27] M. Watanabe, H. Igarashi, K. Yosioka, Electrochim. Acta 40 (1995) 329–334.
[28] T.J. Schmidt, H.A. Gasteiger, G.D. Stab, D.M. Urban, R.J. Behm, J. Electrochem. Soc. 145 (1998) 2354–2358.
[29] U.A. Paulus, A. Wokaun, G.G. Scherer, T.J. Schmibt, V. Stamenkovic, V. Radmilovic, N.M. Markovic, P.N. Ross, J. Phys. Chem. B 106 (2002) 4181–4191.
[30] I. Dutta, M.K. Carpenter, M.P. Balogh, J.M. Ziegelbauer, T.E. Moylan, M.H. Atwan, N.P. Irish, J. Phys. Chem. C 114 (2010) 16309–16320.
[31] J. Koutecky, V.G. Levich, Zh. Fiz. Khim. 32 (1958) 1565–1575.
[32] H.R. Colon-Mercado, B.N. Popov, J. Power Sources 155 (2006) 253–263.
[33] S.M. Unni, V.M. Dhavale, V.K. Pillai, S. Kurungot, J. Phys. Chem. C 114 (2010) 14654–14661.
[34] H. Naohara, T. Yoshimoto, N. Toshima, J. Power Sources 195 (2010) 1051–1053.
[35] J. Solla-Gullon, P. Rodriguez, E. Herrero, A. Aldaz, J.M. Feliu, Phys. Chem. Chem. Phys. 10 (2008) 1359–1373.
[36] K.S. Han, O.H. Han, Electrochim. Acta 47 (2001) 519–523.
[37] S. Garbarino, A. Ponrouch, S. Pronovost, J. Gaudet, D. Guay, Electrochem. Commun. 11 (2009) 1924–1927.
[38] R. Gómez, J. Clavilier, J. Electroanal. Chem. 354 (1993) 189–208.
[39] K. Kinoshita, J. Electrochem. Soc. 137 (1990) 845–848.
[40] A.Y. Stakheev, L.M. Kustov, Appl. Catal., A 188 (1999) 3–35.
[41] S. Mukerjee, J. McBreen, J. Electroanal. Chem. 448 (1998) 163–171.
[42] Y. Takasu, N. Ohashi, X.G. Zhang, Y. Murakami, H. Minagawa, S. Sato, K. Yahikozawa, Electrochim. Acta 41 (1996) 2595–2600.
[43] J.J. Wang, G.P. Yin, Y.Y. Shao, S. Zhang, Z.B. Wang, Y.Z. Gao, J. Power Sources 171 (2007) 331–339.
[44] O.V. Cherstiouk, A.N. Simonov, N.S. Moseva, S.V. Cherapanova, P.A. Simonov, V.I. Zaikovskii, E.R. Savinova, Electrochim. Acta 55 (2010) 8453–8460.
[45] R. Jinnouchi, E. Toyoda, T. Hatanaka, Y. Morimoto, J. Phys. Chem. C 114 (2010) 17557–17568.
[46] A.I. Danilov, E.B. Molodkina, Y.M. Polukarov, Russ. J. Electrochem. 40 (2004) 585–596.
[47] Z.H. Gu, P.B. Balbuena, J. Phys. Chem. C 111 (2007) 9877–9883.
[48] H. Yang, W. Vogel, C. Lamy, N. Alonso-Vante, J. Phys. Chem. B 108 (2004) 11024–11034.
[49] M. Inaba, H. Yamada, J. Tokunaga, A. Tasaka, Electrochem. Solid-State Lett. 7 (2004) A474–A476.
[50] A. Ohma, S. Suga, S. Yamamoto, K. Shinohara, J. Electrochem. Soc. 154 (2007) B757–B760.